Technical Validation of the Zeto Wireless, Dry Electrode EEG System

Z. Nadasdy[1,2,3], A.S. Fogarty[4], R.S. Fisher[4], C.T. Primiani[4], and K. Graber[4]

***Abstract*— *Objective:* Clinical adoption of innovative EEG technology is contingent on the non-inferiority of the new devices relative to conventional ones. We present the four key results from testing the signal quality of Zeto's WR19 EEG system against a conventional EEG system conducted on patients in a clinical setting. *Methods:* We performed 30-minute simultaneous recordings using the Zeto WR19 (zEEG) and a conventional clinical EEG system (cEEG) in a cohort of 15 patients. We compared the signal quality between the two EEG systems by computing time domain statistics, spectral density, and signal-to-noise ratio. *Results:* All the statistical comparisons resulted in signal quality non-inferior relative to cEEG. (i) Time domain statistics, including the Hjorth parameters, showed equivalence between the two systems, except for a significant reduction of sensitivity to electric noise in zEEG relative to cEEG. (ii) The point-by-point waveform correlation between the two systems was acceptable (r>0.6; P<0.001). (iii) Each of the 15 datasets showed a high spectral correlation (r>0.99; P<0.001) and overlapping spectral density across all electrode positions, indicating no systematic signal distortion. (iv) The mean signal-to-noise ratio (SNR) of the zEEG system exceeded that of the cEEG by 4.82 dB, equivalent to 16% improvement. *Conclusion:* In terms of signal quality, the zEEG system is non-inferior to conventional clinical EEG systems with respect to all relevant technical parameters that determine EEG readability and interpretability. *Significance:* Zeto's WR19 wireless dry electrode system has signal quality in the clinical EEG space equivalent to traditional cEEG recordings.**

***Index Terms*—EEG, signal quality, Hjorth parameters, electrophysiology, signal-to-noise ratio, spectral density, dry electrodes, wearable sensors.**

I. Introduction

Wireless technology is transforming the practice of electroencephalography (EEG), yet a smooth transition to the new technology is contingent upon uncompromised data quality [1]. Therefore, a thorough technical validation of a new EEG instrument is critical to clinical adoption. Zeto introduced a wireless dry electrode system, consisting of the WR19 headset and software platform, to improve accessibility, turnaround times, user convenience, patient comfort and experience. It provides easy setup/removal and real-time remote monitoring an FDA 510(k) clearance in 2018 based on clinical studies that demonstrated non-inferiority to a conventional clinical EEG system. Here, we are reporting the results of a study conducted by an independent team of physician experts from the Department of Neurology and Neurological Sciences of Stanford, who integrated the Zeto WR19 system in their routine clinical exam by using it simultaneously with a conventional device as a reference.

In the typical process of setting up an EEG recording using conventional equipment, a trained technologist measures the head, marks electrode locations, abrades the skin, and applies paste and electrodes to the scalp, eventually tethering the patient to a box with wires. This procedure consumes time, requires technologists who need to be perpetually on call, and puts patients through a needlessly uncomfortable experience. The scarcity of technologists makes the problem worse, even unfeasible in many hospitals, emergency rooms, and other outpatient settings. Essential features such as easy data sharing and remote interpretation remain unavailable.

Zeto's EEG Platform (zEEG) provides an FDA-cleared, commercially available, minimal-prep, wireless, dry electrode alternative to the conventional EEG that can be used to perform a clinical EEG anywhere. Data is streamed to a secure cloud platform that provides live display. The zEEG system also provides tools for analysis and optional remote interpretation by neurologists. The WR19 headset uses soft gel-tip electrodes that do not require skin preparation or electrode paste, are dry to the touch, and leave no residue. Hence, the setup time is typically under 5 minutes, with the single-use disposable electrodes making patient clean-up and turnaround time much quicker. In addition to providing soft contact, the soft tips and flexible wires on the electrodes improve the stability of the electrode-to-skin interface.

The advantages of dry electrodes in reducing preparation time are broadly recognized. Many publications demonstrate the competitive performance of dry electrodes relative to conventional systems [2-11]. While dry electrodes significantly improve patient comfort and reduce the EEG preparation time, they pose technical challenges that need to be solved with complete system engineering.

Because signal equivalence is pivotal for clinical interpretability, the zEEG system leveraged four key innovations to protect signal quality: *signal conditioning*, *noise shielding and cancellation, increased signal resolution*, and *artifact management*:

Signal conditioning: Since the magnitude of EEG signal is of the order of μV, it is susceptible to external noise. EEG signals on the scalp are weak as the outer layer of the skin, the 'epidermis,' presents a high impedance path [10,12]. These signals are too weak to drive through a long wire (several feet) to reach the amplifier box. Hence, before placing the electrodes, EEG technologists abrade the skin surface (effectively

The paper was submitted for review on 04/16/2024. Z.N. Author is with the [1]Zeto, Inc., Santa Clara, CA; [2] UT Austin, Austin TX; [3] Eötvös Loránd University, Budapest, Hungary. Authors A.S.F., R.S.F., C.T.P. and K.G. are with the [4]Department of Neurology and Neurological Sciences, Stanford University, Palo Alto, CA. (correspondence e-mail: zoltan@utexas.edu). Z.N. and R.S.F. hold stock options in Zeto. The WR19 headsets and electrodes were provided by Zeto, Inc., Santa Clara, CA.

scratching away the epidermis layer) and apply a conductive paste to lower the skin impedance to 10 KΩ. Therefore, in conventional EEG systems, the impedance needs to be constantly monitored to be at or below the 10 KΩ threshold; otherwise, electrical interference would contaminate the signal. The zEEG headset was designed to circumvent the skin preparation by placing pre-amplification close to the electrodes. The pre-amp (front-end amplifier) converts the signal from a weakly driven, high-impedance input to a strongly driven, low-impedance output with precise gain matching between amplifiers, matched to the level of 5 x 10^{-4}. This provides extremely high input impedance (1 TΩ) and low leakage current (< 0.5 pA). Once amplified, the signals are less susceptible than passive electrode systems to pick up external noise. This enables dry electrodes to work with minimal skin preparation.

Noise shielding and cancellation: The zEEG headset employs noise shielding to protect the signal from external interference through several proprietary methods. In addition, active noise cancellation enables further improvement in signal quality.

Signal resolution: The zEEG headset utilizes the latest generation 24-bit ADC, which offers superior range (± 350 mV) and exceptional linearity. The amplitude of the common mode signal can be as high as several volts, while EEG is in the range of several tens of microvolts. Hence, at least 100 dB of Common Mode Rejection Ratio is essential. Therefore, the data acquisition systems must suppress common mode voltage down to a few microvolts while the bioelectric signal (differential mode signal) must be amplified [13]. To achieve that, the zEEG headset uses a patent-pending active common mode cancellation technique. This technique dynamically calculates the average common mode voltage and applies negative feedback that cancels out the common mode voltage appearing in every channel.

Artifact management: One of the biggest concerns with dry electrodes is their sensitivity to movement-related artifacts. Conventional wet electrodes eliminate this problem by being glued to the scalp. The conductive paste also acts as a shock absorber, minimizing relative motion between the electrode and scalp, thereby reducing motion artifacts. In the zEEG headset, the mechanical design minimizes relative motion between electrode and scalp via a carefully engineered helmet, using adjustable bands, spring-loaded and flexible electrodes with soft gel tips. These mechanisms work synergistically to ensure each electrode stays in contact with the skin despite motion.

Each of these methods can improve the quality of EEG, but their combined effect significantly reduces systematic noise. As a result, the signal-to-noise ratio (SNR) of zEEG headset exceeds the SNR of conventional EEG (see Results).

This study focuses on four features of equivalence:

1. Time domain statistics: We compared the Hjorth parameters, artifact prevalence, baseline wander and electric noise susceptibility between the two systems.
2. Point-by-point amplitude correlation: We tested the correlation between the zEEG and cEEG waveforms. Technically, we measured the voltage of the two corresponding signals at each t_i sampling point in μV and computed the correlation between the sequences of measurements over an interval of $t_{i..n}$ for each electrode position.
3. Spectral-domain correlation: We computed the spectral density in sliding windows per electrode and expressed the correlation between the two continuous power spectra.
4. Signal-to-noise ratio (SNR) estimate: We defined the SNR at each data point of both time series per electrode position. Then, we compared the SNR distributions between the two systems at each electrode position using multiple t-tests.

We set up the following acceptance criteria for equivalence:

1. Time domain statistics are considered statistically equivalent between the two types of EEG recordings if, based on non-parametric statistics, such as Wilcoxon's signed rank test, we cannot reject the null hypothesis.
2. The point-by-point amplitude correlation must demonstrate a visually compelling similarity of waveforms by overlaying the zEEG and cEEG data on a shared μV axis separately for every electrode position. The similarity has to be quantified by computing the point-by-point Pearson's correlations between the corresponding EEG data for all electrode positions. Pearson's r > 0.5 will be acceptable, considering the necessary spatial separation between the corresponding electrode pairs (see Methods and Discussion).
3. We consider the zEEG and cEEG power spectra equivalent if the average spectral density +/- standard deviation overlaps along the clinically relevant 0.1 to 80 Hz frequency range. In addition, Pearson's correlation coefficient between the mean spectral density curves should exceed 0.9 to recognize the two recordings as equivalent in the spectral domain.
4. We consider the two SNR equivalent if the aggregated SNR distribution of zEEG and that of the cEEG are statistically indistinguishable using a one-sample t-test. Since the null hypothesis of the test is equivalence, the rejection of the null indicates the superior performance of one system over the other in terms of SNR.

II. Methods

To compare the EEG signals between the cEEG (Nihon-Kohden JE-921A system) and zEEG (Zeto WR19 wireless headset), we simultaneously recorded 30-minute duration EEGs from fifteen patients at the Department of Neurology & Neurological Sciences at Stanford. All patients have consented under the Stanford IRB's oversight (eProtocol #: 61767, Approval Date: January 30, 2023).

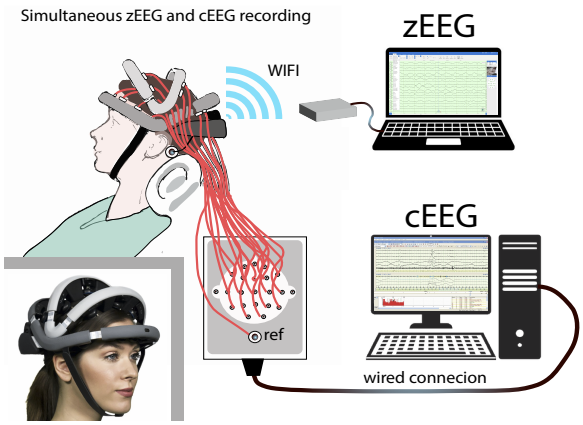

Figure 1: The set-up of simultaneous recordings in clinical environments. Patients were leaning back in a comfortable position while the Zeto WR-19 headset was positioned first, followed by arranging the gel-loaded clinical electrodes as close as possible to the Zeto electrodes. All recordings yielded clinically interpretable signals on all electrodes. The inset at the lower left is a photograph of the WR19 headset.

The zEEG system uses proprietary active electrode technology and cloud-based software (the Zeto Cloud Platform). First, the zEEG headset was placed on the participant's head, electrodes by design positioned according to the international 10-20 convention, and the headset was fastened using a chinstrap. The electrode contact quality was checked, and only after good contact quality was confirmed for all electrodes did the EEG technologist attach the cEEG electrodes. The skin area next to the zEEG electrodes, approximately 1 cm away was cleaned with NuPrep. The electrodes used in the cEEG were disposable Ag/AgCl cup electrodes loaded with Ten20 conductive paste and attached to the skin with adhesive medical tape. The cEEG electrodes were placed approximately 1 cm posterior to the zEEG electrodes to avoid an electric bridge between them. Subjects sat in a reclined chair with a back pillow or neck roll (Fig. 1). The sampling rate of zEEG and cEEG systems were set to 250 and 200 sample/s, respectively.

As part of the time-domain comparison, we computed the Hjorth parameters: activity, mobility, and complexity. These parameters were introduced by Bo Hjorth [14] to indicate whether the EEG is fit for feature extraction.

The activity parameter represents the signal power as the variance of the signal:

$$Activity = var\big(y(t)\big),$$

where y(t) represents the time-varying signal.

The mobility parameter is the square root of the ratio of the variance of the first derivative of the signal to that of the signal. This parameter expresses the mean frequency or the proportion of the standard deviation of the power spectrum.

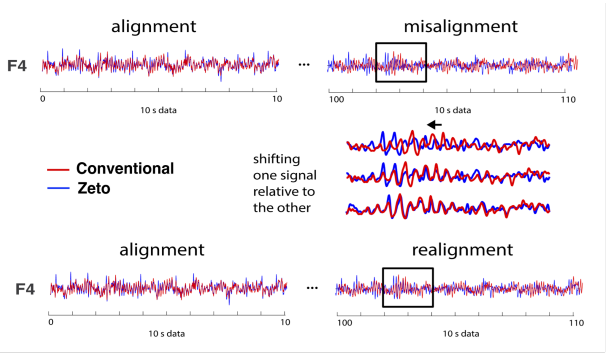

Figure 2: The method of adaptive alignment of the signals recorded by the Zeto and the conventional EEG system. The plots on the top show two 10 s EEG signals recorded from channel-F4 at the beginning of the recording and 100 s later. During the recording, a drift occurred as expected between the clocks of the two independent EEG systems resulting in an offset between the two signals (top right). Using 10 s time windows we calculated the signal-to-signal correlation between the two recordings, and we added variable delays between -200 to + 200 ms to one of the signals and re-calculated the correlations. We used a DT correction that resulted in the best correlation between the two EEGs and applied that correction to the entire 10 s data. The algorithm then recursively computed the delay between the subsequent 10 s data segments.

$$Mobility = \sqrt{\frac{var\left(\frac{dy(t)}{dx}\right)}{var(y(t))}}.$$

The complexity parameter represents the change in frequency. It expresses the signal's similarity to a pure sine wave when its value converges to 1.

$$Complexity = \frac{mobility\left(\frac{dy(t)}{dt}\right)}{mobility(y(t))}.$$

In addition, we computed the kurtosis, i.e., the ''tailedness" of the amplitude probability distribution. Kurtosis is the fourth moment of the signal and characterizes the deviation of the amplitude distribution from the standard-normal distribution, which is the signature of an artifact-free EEG. Kurtosis is defined as:

$$Kurtosis = E\left[\left(\frac{y-\mu}{\sigma}\right)^4\right],$$

where y is the time-domain signal, μ is the mean of y, σ is its standard deviation and E is the expected value of y. Kurtosis measures the prevalence of outliers. For instance, if the distribution has a Kurtosis>3 ("leptokurtic"), the signal contains a substantial number of outliers.

Another measure of the prevalence of outliers was the artifact ratio. Artifacts were defined as the fraction of data points with an absolute value > 6 STD from the mean. Kamousi et al. [15] introduced this metric, which we adopted for comparison.

Moreover, we computed a "baseline wander" parameter to quantify the change of the average baseline drift that occurred between successive 10 s segments over the whole EEG, also adopted from [15].

As the last parameter in the time domain statistics, we computed the average power of 60 Hz electrical noise interference with the unfiltered EEG signal between 59 and 61

Hz. AC electrical noise contaminates the signal arising from brain's intrinsic gamma oscillations, which holds diagnostic utility. Hence, susceptibility to this noise is an important metric for comparing EEG systems as it indicates the efficacy of system engineering.

We compared all the above-described metrics between the two systems by averaging each parameter across the 19 electrode positions and computing the within-subject differences using Wilcoxon's signed rank tests.

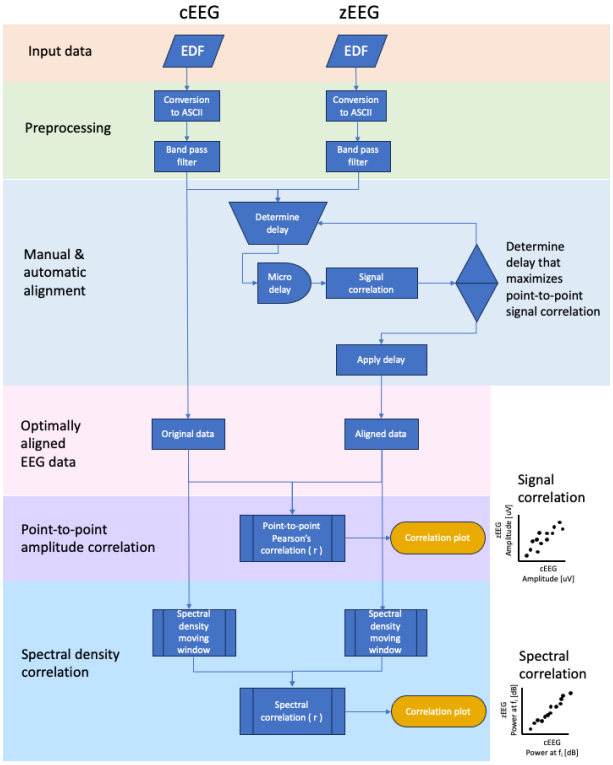

Figure 3: The pipeline of data processing. The same data processing steps were applied to both EEG recordings except the adaptive realignment applied to the zEEG data stream. (It does not matter which system we applied the adaptive realignment.) We computed two main outputs, and plotted the signal correlations and from the spectral analysis we plotted the spectral correlations.

The most compelling demonstration of signal equivalence is the visual comparison of the two simultaneous waveforms recorded from adjacent electrodes. A point-by-point amplitude comparison requires perfect temporal and amplitude alignment between the two EEG samples. To achieve that, the amplitudes were displayed relative to a common μV scale using referential montages for both systems. The temporal alignment involved multiple steps. First, to match the sampling rates, we up-sampled the cEEG data from 200 Hz to 250 Hz using Matlab's (Mathworks, Natick, MA) cubic-spline interpolation method. To enable a rudimental offline synchronization between the two recordings, we asked each participant to make five consecutive blinks at the beginning of the recording, and we used those blinking artifacts as markers to align the recordings. In order to precisely align the two signals at sampling precision (4 ms) and maintain their synchrony over time, we introduced an adaptive alignment method (Fig. 2). Briefly, we divided both EEG data sets into 10 s nonoverlapping segments. Then, we shifted the entire zEEG data (all channels) in time from -80 to +80 ms in 4 ms steps and computed the correlation between all corresponding data points within that segment. The average correlation over the 19 electrodes was the signal correlation for that specific time shift. Next, we repeated the process with incremental time shifts until completion of the full 160 ms range and identified the single time shift associated with the 160 ms long correlation curve. We realigned the zEEG relative to cEEG by applying the shift (usually not more than two sampling points) that provided the highest correlation for the given segment and iterated the process for all other segments (Fig. 3). This method compensated for the occasional sample drifts that could occur due to independent clock signals and kept the two samples synchronized over the entire duration of recordings. While this adaptive realignment was crucial for estimating the signal correlation, the number of such realignments was negligible. This method allowed for computing a direct point-by-point correlation, spectral correlation, and signal-to-noise (SNR) estimations.

To compare the spectral characteristics of signal transmission between the zEEG and cEEG systems, we used a sliding-window implementation of the power spectral density estimate (Matlab, Mathworks, Natick, MA) with 10 s overlapping windows. The spectral density function was smoothened by a moving average of two points for each time window and averaged across all time windows to obtain a mean spectral density function and standard deviation (STD). We computed Pearson's correlation coefficients of the zEEG and cEEG average spectral density functions between corresponding frequencies at 0.1 Hz resolution.

Because signal and spectral correlations can only estimate the equivalence/non-equivalence of the two systems but do not determine which system performs better, we sought a method to estimate signal quality at a common scale. The signal-to-noise ratio provides an estimate of the fidelity of the signal and allows for a direct comparison of the two systems. The challenge is to work out an objective method to separate the noise from the signal in the EEG data because we do not have direct access to the intra-cortical dipoles that underlie the signal, which propagates to the surface and manifests as scalp EEG. As an alternative, we can utilize an unsupervised artifact reduction algorithm that removes the noise from EEG recordings and allows for estimating the noise as the difference between the original and the artifact-reduced EEG. The method is unbiased if we apply the same noise removal algorithm to both EEG data. We utilized 'PureEEG,' an FDA-cleared[1] digital artifact reduction (AR) software module based on a stochastic, spatio-temporal model for EEG, developed by Encevis (AIT, Austria) [16], which inputs the original raw EEG and outputs the artifact-reduced estimate of the same EEG. Even if the AR method was imperfect, as it might have altered the true signal, applying it to both EEG recordings affects both signals to the same extent. To calculate SNR, we considered the AR signal to represent the "true signal" and the difference between the "true signal" and the original raw EEG as "noise."

[1] Reference to Encevis' FDA 510(k) approval letter: https://www.accessdata.fda.gov/cdrh_docs/pdf17/K171720.pdf

Then, we computed the SNR for both systems at each electrode position separately (Fig. 4). The average channel-by-channel SNR was considered as the mean SNR of a given system and compared to the mean SNR of the other system. This method provided a relatively unbiased estimate of the signal quality in dB for both systems.

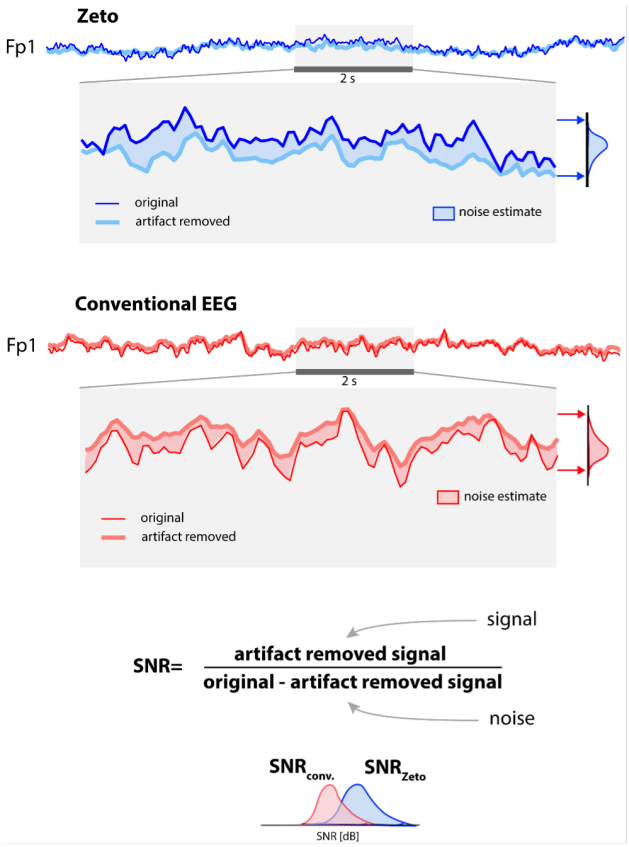

Figure 4: The method of calculating the signal-to-noise ratios for the two systems. The top panel illustrates a 5 s sample of raw EEG recorded by the zEEG system and same signal after artifact reduction. The difference is depicted by the bell-shaped distribution on the right. The bottom panel is the same for the cEEG system. The equation defines the calculation of SNR. The SNR is expressed in dB units; hence it allows for direct comparison between the two systems. The average SNR difference expresses the distances between the SNR distributions of the two EEG systems.

III. Results

Data were analyzed from all 15 patients enrolled, ages between 19 and 70 years old; seven of them were females. All 15 recordings resulted in acceptable quality EEG signals for 90% of the total recording duration on all 19 electrodes, and 10% were unreadable due to artifacts in both systems (this proportion of artifacts is typical due to involuntary movements and verbal interactions with the patients during the recording). Interpretations from cEEG included abnormal (n=3), diffusely slow (n=1), and focally slow (n=1), with none showing ictal activity.

The analysis of time-domain statistics revealed no significant difference between the zEEG and cEEG systems in all metrics we tested except the sensitivity to electric noise (Table 1). The zEEG system showed a significant reduction of 60 Hz power line interference with the signal (p=0.0003) relative to the cEEG, an effect attributable to the driven analog (EEG) signal and noise shielding in the Zeto WR19 headset.

Parameter		Mean zEEG	Mean cEEG	P
Hjorth	Activity	7748.4	4074.18	0.0832
	Mobility	0.1308	0.1648	0.0637
	Complexity	4.1175	3.5492	0.0637
Artifact Ratio		0.0035	0.0029	0.1688
Curtosis		570.23	1060.29	0.4543
Baseline wander		1.4045	0.9526	0.0833
Electric noise		5.349	15.1338	0.0003 ***

Table 1. Comparison of non-spectral EEG quality indicators. Parameter definitions are in the text. The P statistics were obtained by using Wilcoxon's signed rank test, a non-parametric test for comparing rank-ordered data. Only electric noise showed a significant difference, in favor of zEEG.

None of these metrics can substitute for the direct visual comparison of a 10 s sample of two EEGs displayed in a superimposed fashion, including all 19 electrodes (Fig. 5). Note the substantial overlap between the EEG waveforms.

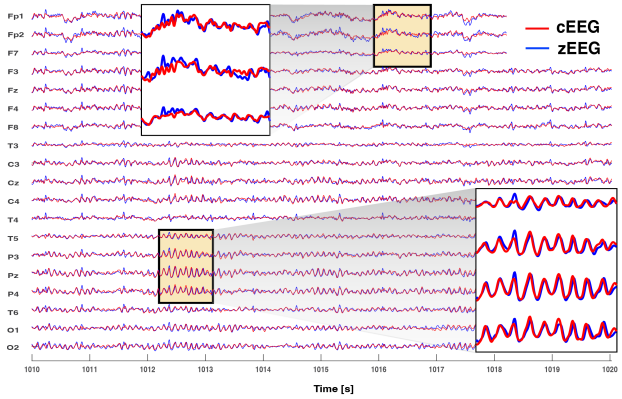

Figure 5: Direct signal-to-signal comparison. The two simultaneous 10 s EEG samples of Zeto and NK system overlaid after resampling and adaptive realignment. The match between the two recordings on all 19 electrodes is apparent. Insets represent details on a magnified scale.

To substantiate the visual assertion of similarity, we computed the point-by-point correlation between pairs of waveforms for the complete 30-minute recordings for each participant. None of our datasets showed a less than 0.6 Pearson's correlation coefficient (r>0.6; P<0.001), even though the two systems were not recorded at the same sampling frequency and electrodes were 1-2 cm apart (Fig. 5).

Because relevant clinical information is concealed in the spectral domain, it is critical to assert any systematic discordance in spectral characteristics between the two systems. Therefore, we compared the mean and standard deviation of spectrograms computed across 10 s sliding windows (Fig. 6). The overlap between the STD bands around the mean spectral density curves suggests no systematic spectral difference between zEEG and cEEG in the 0.1-80 Hz range (Fig. 6,7). The

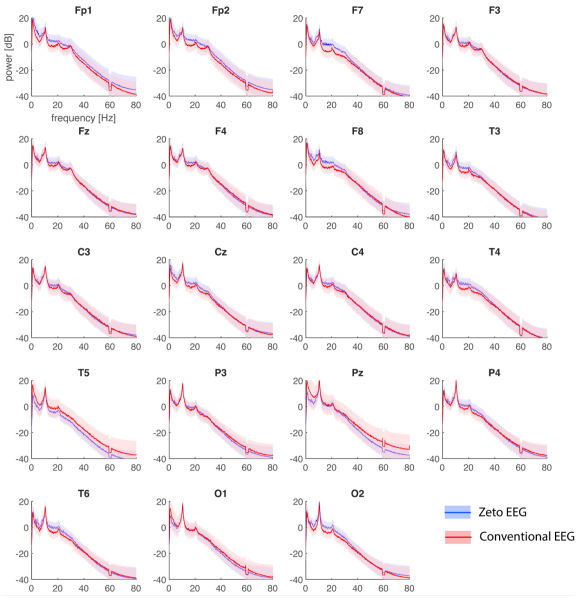

Figure 6: Spectral analysis of simultaneous recordings. The channel-by-channel average spectral density and Standard Error of the mean is shown as shaded areas around the mean. Spectral analysis was calculated in 10 s sliding windows by using multi-taper method. Notice the 60 Hz notch filtering artifact, and the posteriorly maximal alpha power peak. Both the mean spectral density as well as the standard error qualitatively show a close match between the two systems.

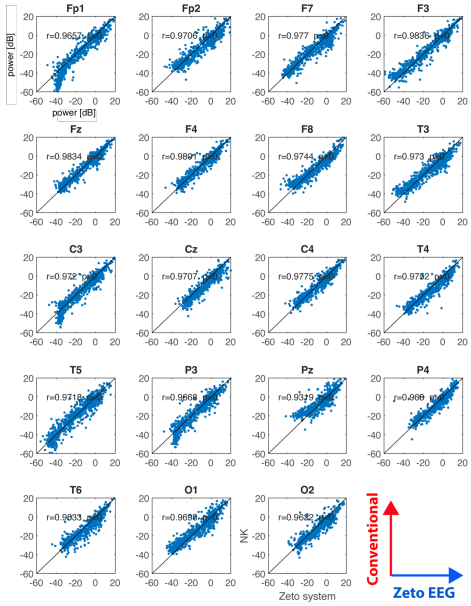

Figure 7: Spectral correlations. Spectral correlations at different electrode positions from a single participant. Each data point represents the average power in [dB] at the same specific frequency in both EEG systems.

population-wide distributions of spectral correlations were consistently high (Pearson r>0.995) at each electrode position (Fig. 8).

While the point-by-point and spectral correlations indicated substantial agreement between the two EEG records, the correlations do not inform which recording system is more sensitive to signals originating from the brain. Therefore, we introduced a method to quantify the signal-to-noise ratio (SNR) of the two systems by estimating the contribution of noise to the signal (See Methods and Fig. 4). We found that the mean SNR of zEEG averaged over electrode positions exceeded the SNR of cEEG by an average of 4.8176 dB, which accounted for 16 % signal improvement (Fig. 9).

This difference in SNR in favor of zEEG was significant at all the 19 electrode positions ($Tstat_{min}$=119.49, P<0.001; $Tstat_{max}$=734.16; P<0.000; df=383599) no matter whether we analyzed the entire 30-minute recording with artifacts included or only a 90 s long artifact-free interval (Fig. 9 upper and lower panel, respectively).

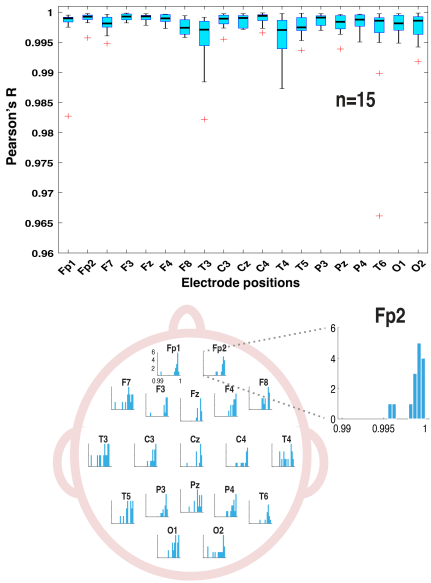

Figure 8. Spectral Correlations computed across all subjects. The top part shows a box-plot representation of spectral correlation values per channel. Horizontal lines in the middle of boxes are medians, and the size of the box represents the upper and lower first quartiles. The bottom part depicts the correlations as histograms projected according to the electrode topography overlaid on a head model.

Discussion

Dry electrode wireless EEG systems challenge the status quo of conventional EEG in many features, including signal quality and clinical interpretability, whether used in clinical neurology, experimental psychology, or neuroscience. Our analysis demonstrates that innovative features when synergistically applied, can close the gap and eventually exceed the signal quality of standard clinical EEG systems. This study compared the most important performance metrics of EEG between a novel and a conventional recording device, including time domain statistics, point-by-point signal correlation, spectral domain statistics, and SNR. The time domain analysis determines the statistical equivalence of the signal dynamics expressed by the Hjorth parameters. The point-by-point correlation asserts the waveform similarity between the two systems, which is critical for detecting and classifying clinical events in the EEG. The comparison of spectral density statistics can articulate subtle differences between EEG systems in their

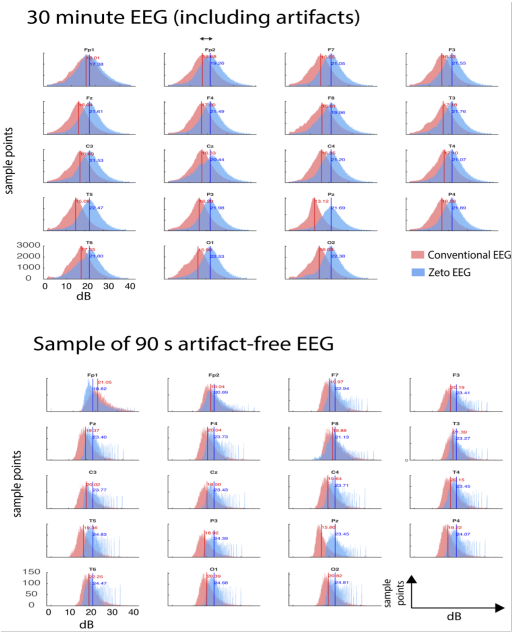

Figure 9: The observed SNR differences per electrode position. The top panel represents the SNR distributions of zEEG (blue) and cEEG (pink) systems overlaid for each channel separately. The SNR distributions were computed from the entire 30-minute EEG recordings of one subject. The bottom panel represents the SNR distributions computed from the same recording but from a 90 s artifact-free EEG with the same color code as the top panel. Numbers in blue and red represent the medians of the zEEG and cEEG SNR distributions, respectively.

sensitivity to periodic components of neuronal activity in the delta, theta, alpha, beta, and gamma bands of the EEG. These oscillations have diagnostic relevance, and their prominence is a mandatory part of clinical EEG reports. Lastly, using SNR we compare the performance of zEEG to that of cEEG, which promises to serve as a benchmark for future tests.

To make an unbiased comparison of EEG signals, we used simultaneous EEG recordings as a gold standard. We included all 19 electrodes per system (38 electrodes plus references) according to the 10-20 arrangement by placing them as close as possible without touching each other, typically about 1 cm apart. This ensured that the recording conditions were identical, and the data sampling was balanced at 250 samples/s between both systems (Table 2). Both temporal and spectral statistics resulted in significant concordances between the two EEG systems despite the spatial separation of electrodes.

The method of simultaneous recordings also has its own intrinsic caveats due to the spatial scale at which EEG signal changes over the surface of the scalp. Cortical activity dynamics consists of propagating waves at different frequencies that change the signal's amplitude at a sub-centimeter scale in the brain [17,18]. Therefore, we cannot expect to record the same signal from adjacent electrodes. In addition, the reference electrodes were placed at different positions (linked mastoid A1-A2 for Zeto and Cz-Pz for the NK system), which also rendered a difference in signal amplitude distribution (Table 2). Moreover, the impedance of the electrodes and the susceptibility to electrical noise were different between the two systems. The zEEG system used active electrode technology, noise shielding, and 24-bit Analog to Digital Conversion (ADC) resolution; the NK system used passive electrodes and 16-bit ADC resolution (Table 2). Despite factors that made the two recording conditions different, we found a significant match between the two systems across all investigated metrics (Table 2). This comparison demonstrates that the Zeto zEEG system is non-inferior to the conventional cEEG system with respect to signal quality and efficacy.

Finally, the SNRs calculated based on the artifact reduction algorithm enabled us to compare the two systems parametrically. The SNR values were expressed in dB, and the two systems were compared on complete 30-minute as well as short (90 s) artifact-free segments. Under both conditions, we found the zEEG displaying higher SNR at all electrode positions than the cEEG (Table 2). This comparison strongly supports the claim that innovative, well-engineered systems such as the zEEG can produce an EEG signal exceeding the quality of conventional EEG, despite the higher impedance of unprepared skin relative to cEEG.

	Zeto WR19	N-K JE-921A	Concordance	Difference
Electrodes	Ag coated plastic with soft gel tip	Ag/AgCl with conductive gel		
Electrode contact type	Touching the skin	Glued to the skin with adhesive tape		
Skin impedance	1TΩ	20 kΩ		
Sampling frequency	250 Hz	200 Hz (250 Hz up sample)		
Bit resolution	24	16		
Amplifiers	active	passive		
Electrode shielding	shielded	non-shielded		
Coverage	Full montage, 19 electrodes	Full montage, 19 electrodes		
Recording References	Linked mastoid, A1-A2	Cz-Pz		
Line-noise artifact filtering	59-61 Hz	59-61 Hz		
Bandpass filtering	0.5-59 Hz	0.5-59 Hz		
Hjorth parameters	Activity=7748.4 Mobility=0.1308 Complexity=4.1175	Activity=4074.18 Mobility=0.1648 Complexity=3.5492	P=0.0832 P=0.0637 P=0.0637	
Signal correlation	Point-by-point	Point-by-point	Pearson's r=0.46-0.94 P<0.001	
Spectral correlation	Between 0.5 and 59 Hz	Between 0.5 and 59 Hz	Pearson's r>0.99 P<0.00001	
SNR	20.15 dB	15.33 dB		P<0.001

Table 2: Summary of system parameters and results. The first column summarizes the parameters relevant for comparing the two systems (white field). The second and third columns provide the actual values of those parameters for the zEEG (Zeto) and cEEG (Nihon-Kohden) systems in blue and pink, respectively. The bottom of the table summarizes the study results: the Hjorth parameters, the mean signal correlation, the mean spectral correlation, and the median differences between the signal-to-noise ratio estimates.

REFERENCES

[1] Niso G, Romero E, Moreau JT, Araujo A, Krol LR. Wireless EEG (2023). A survey of systems and studies. Neuroimage. 269:119774. doi: 10.1016/j.neuroimage.2022.119774. Epub 2022 Dec 22. PMID: 36566924.

[2] Guger, C., Krausz, G., Allison, B., & Edlinger, G. (2012). Comparison of Dry and Gel Based Electrodes for P300 Brain–Computer Interfaces. Frontiers in Neuroscience, 6, 60. https://doi.org/10.3389/fnins.2012.00060

[3] Di Flumeri, G., Aricò, P., Borghini, G., Sciaraffa, N., Di Florio, A., & Babiloni, F. (2019). The Dry Revolution: Evaluation of Three Different EEG Dry Electrode Types in Terms of Signal Spectral Features, Mental States Classification and Usability. Sensors (Basel, Switzerland), 19(6), 1365. https://doi.org/10.3390/s19061365

[4] Fiedler, P., Haueisen, J., Jannek, D., Griebel, S., Zentner, L., Vaz, F., & Fonseca, C. (2014). Comparison of three types of dry electrodes for electroencephalography. In Acta IMEKO. https://doi.org/10.21014/acta_imeko.v3i3.94

[5] Hinrichs, H., Scholz, M., Baum, A. K., Kam, J. W. Y., Knight, R. T., & Heinze, H. J. (2020). Comparison between a wireless dry electrode EEG system with a conventional wired wet electrode EEG system for clinical applications. Scientific Reports. https://doi.org/10.1038/s41598-020-62154-0

[6] Kam, J. W. Y., Griffin, S., Shen, A., Patel, S., Hinrichs, H., Heinze, H.-J., … Knight, R. T. (2019). Systematic comparison between a wireless EEG system with dry electrodes and a wired EEG system with wet electrodes. NeuroImage, 184, 119 129. https://doi.org/10.1016/j.neuroimage.2018.09.012

[7] Leach, S., Chung, K., Tüshaus, L., Huber, R., & Karlen, W. (2020). A Protocol for Comparing Dry and Wet EEG Electrodes During Sleep. Frontiers in Neuroscience, 14,586. https://doi.org/10.3389/fnins.2020.00586

[8] Li, G.-L., Wu, J.-T., Xia, Y.-H., He, Q.-G., & Jin, H.-G. (2020). Review of semi-dry electrodes for EEG recording. Journal of Neural Engineering, 17(5), 51004. https://doi.org/10.1088/1741-2552/abbd50

[9] Mathewson, K. E., Harrison, T. J. L., & Kizuk, S. A. D. (2017). High and dry? Comparing active dry EEG electrodes to active and passive wet electrodes. Psychophysiology, 54(1), 74-82. https://doi.org/10.1111/psyp.12536

[10] Shad, E. H. T., Molinas, M., & Ytterdal, T. (2020). Impedance and Noise of Passive and Active Dry EEG Electrodes: A Review. IEEE Sensors Journal, 20(24),

[11] Zander, T., Lehne, M., Ihme, K., Jatzev, S., Correia, J., Kothe, C., … Nijboer, F. (2011). A Dry EEG-System for Scientific Research and Brain–Computer Interfaces. Frontiers in Neuroscience, 5, 53. https://doi.org/10.3389/fnins.2011.00053

[12] Lopez-Gordo, M.A.; Sanchez-Morillo, D.; Valle, F.P. (2014). Dry EEG Electrodes. Sensors 2014, 14, 12847–12870.

[13] Guermandi M, Scarselli EF, Guerrieri R. A (2016). Driving Right Leg Circuit (DgRL) for Improved Common Mode Rejection in Bio-Potential Acquisition Systems. IEEE Trans Biomed Circuits Syst. 10(2):507-17. doi: 10.1109/TBCAS.2015.2446753. Epub 2015 Aug 14. PMID: 26285217.

[14] Hjorth B. (1970) EEG analysis based on time domain properties. Electroencephalogr Clin Neurophysiol. (3):306-10. doi: 10.1016/0013-4694(70)90143-4. PMID: 4195653.

[15] Kamousi B, Grant AM, Bachelder B, Yi J, Hajinoroozi M, Woo R. (2019) Comparing the quality of signals recorded with a rapid response EEG and conventional clinical EEG systems. Clin Neurophysiol Pract. 4:69-75. doi: 10.1016/j.cnp.2019.02.002. PMID: 30976727; PMCID: PMC6444024.

[16] Hartmann M.M., Schindler K, Gebbink T.A., Gritsch G, Kluge T. (2014) PureEEG: automatic EEG artifact removal for epilepsy monitoring. Neurophysiol Clin. 44(5):479-90. doi: 10.1016/j.neucli.2014.09.001. PMID: 25438980.

[17] Muller, L., Chavane, F., Reynolds, J., & Sejnowski, T. J. (2018). Cortical travelling waves: mechanisms and computational principles. Nature reviews. Neuroscience, 19(5), 255–268. https://doi.org/10.1038/nrn.2018.20

[18] Zhang, H., Watrous, A. J., Patel, A., & Jacobs, J. (2018). Theta and Alpha Oscillations Are Traveling Waves in the Human Neocortex. Neuron, 98(6), 1269–1281.e4. https://doi.org/10.1016/j.neuron.2018.05.019